

time. The glass can still be dissolved even when the solubility limit of the fluid with respect to the crystalline phase is attained (supersaturation). However, at a certain level of concentration (marked as point II in the region of super-saturated fluid) spontaneous crystallization of the zeolite phase occurs, leading to a decrease of the concentration in the hydrothermal fluid. The zeolites are, therefore, synthesized by a process in which the precursor glass is dissolved in the fluid phase and then crystallizes as zeolite.

Crystal growth only occurs in the region of supersaturated fluid. If the isothermal–isobar conditions are carefully maintained during the long duration of the experiment, neither etching of the zeolite crystals nor the formation of a second zeolite phase (by repeated spontaneous crystallization and growth) is observed. From this it can be concluded that the dissolution–crystallization process continues in the range of supersaturated fluid in such a way that the system is self-stabilizing. These are the time-dependent conditions of crystal growth between point II and III (Figure 2). The process will continue as long as there is enough glassy material for the continuous dissolution–crystallization process—if the synthesis process is not interrupted before.

Experimental Section

Glasses of the appropriate zeolite composition (see Table 3) were repeatedly molten for five minutes and quenched and crushed each time in a high-frequency furnace in open carbon crucibles in air (Schunk Kohlenstofftechnik, Germany) at temperatures up to 1800 °C using a blend of the appropriate water-free alkali metal and/or alkaline earth metal

investigated by scanning electron microscopy (SEM). The resulting micrographs were evaluated with the stereo-comparator for crystal indexing and crystallographic analysis.^[8]

Received: May 4, 2001 [Z17048]

Table 3. The chemical composition of the glass precursors of the aluminosilicate 6-ring zeolites.

Zeolite phase	Precursor glass composition ^[a]
faujasite ^[b]	5 Na ₂ O × 6 CaO × 4 MgO × 15 Al ₂ O ₃ × 66 SiO ₂ × 9.6 (Sr, Ba, K ₂)O × 4.8 Fe ₂ O ₃
gmelinite	1 Na ₂ O × 1 Al ₂ O ₃ × 4 SiO ₂ × 0.6 (Ca, K ₂)O
offretite ^[b]	1 K ₂ O × 2 CaO × 2 MgO × 5 Al ₂ O ₃ × 26 SiO ₂ × 1.8 Fe ₂ O ₃
chabazite	1 CaO × 1 Al ₂ O ₃ × 4 SiO ₂ × 0.6 (Li ₂ , K ₂)O
erionite ^[b]	1 Na ₂ O × 2 K ₂ O × 2 MgO × 3 CaO × 8 Al ₂ O ₃ × 54 SiO ₂ × 3.5 Fe ₂ O ₃
levyne	1 Na ₂ O × 5 CaO × 6 Al ₂ O ₃ × 24 SiO ₂

[a] The cations of the additional mixed oxide components are present in equal proportions. [b] Synthesis only possible in the presence of Fe ions.

carbonate, iron oxide, α -alumina, and silicon dioxide (quartz). Visually homogeneous glasses were amorphous according to powder X-ray-diffraction investigations (XRD, Cu_{K α} radiation, Bragg–Brentano geometry). Then, pieces of the glasses (maximum length 4 mm) were placed in copper capsules (about 1 cm³ volume), filled up with distilled H₂O as pressure and reaction medium (water:glass ratio approximately 10:1) and tightly closed. Three of these capsules were placed in a high-pressure autoclave (MRA/112R type, TEM-PRESS research division, USA). The whole system was set under pressure by using distilled water as the pressure medium. The hydrothermal experiments were conducted in a temperature range between 170 and 270 °C for 60 days at a synthesis pressure of 1 kbar. Every experiment was repeated twice. These conditions were chosen based on experience with previous zeolite syntheses using this method.^[3b,c, 5, 9]

The crystalline phases formed at the surface of the glasses were subsequently investigated by XRD and energy-disperse X-ray analysis for chemical composition (EDX), and the crystal morphology was finally

- [1] R. M. Barrer, *The Hydrothermal Chemistry of Zeolites*, 1st ed., Academic Press, London, **1982**.
- [2] a) G. J. Kim, W. S. Ahn, *Zeolites* **1991**, *11*, 745–750; b) M. L. Occelli, H. E. Robson, *Synthesis of Microporous Materials*, Vol. 2, Chapman and Hall, London, **1992**; c) *Molecular Sieves, Science and Technology*, Vol. 1, *Synthesis* (Eds.: H. G. Karge, J. Weitkamp), Springer, Berlin, **1998**.
- [3] a) G. Gottardi, E. Galli, *Natural Zeolites*, Springer, Heidelberg, **1985**; b) H. Ghobarkar, O. Schäf, *Microporous Mesoporous Mater.* **1998**, *23*, 55–60; c) H. Ghobarkar, O. Schäf, *J. Phys. D: Appl. Phys.* **1998**, *31*, 3172–3176.
- [4] O. Chiyoda, M. E. Davis, *Microporous Mesoporous Mater.* **1999**, *32*, 257–264.
- [5] H. Ghobarkar, O. Schäf, U. Guth, *Prog. Solid State Chem.* **1999**, *27*, 29–73.
- [6] *Atlas of Zeolite Structure Types* (Eds.: W. M. Meier, D. H. Olson, C. Baerlocher), 4th ed., Elsevier, London, **1996**.
- [7] a) K. Fischer, *Neues Jahrb. Mineral. Monatsh.* **1966**, 1–13; b) F. Mazzi, E. Galli, *Neues Jahrb. Mineral. Monatsh.* **1983**, 4461–4480; c) S. Merlino, E. Galli, A. Alberti, *TMPM Tschermaks Mineral. Petrogr. Mitt.* **1975**, *22*, 117–129; d) A. Kawahara, H. Curien, *Bull. Soc. Fr. Mineral. Crystallogr.* **1969**, *92*, 250–256; e) J. A. Gard, J. M. Tait, *Acta Crystallogr.* **1972**, *28*, 825–834; f) G. Bergerhoff, W. H. Baur, W. Nowacki, *Neues Jahrb. Mineral. Monatsh.* **1958**, 193–200.
- [8] H. Ghobarkar, *Krist. Tech.* **1977**, *12*, K49–51.
- [9] a) H. Ghobarkar, O. Schäf, P. Knauth, *Ann. Chim. (Paris)* **1999**, *24*, 209–215; b) H. Ghobarkar, O. Schäf, U. Guth, *High Pressure Res.* **2001**, *20*, 45–54.


Which Structural Elements Are Relevant for the Efficacy of Neocarzinostatin?*

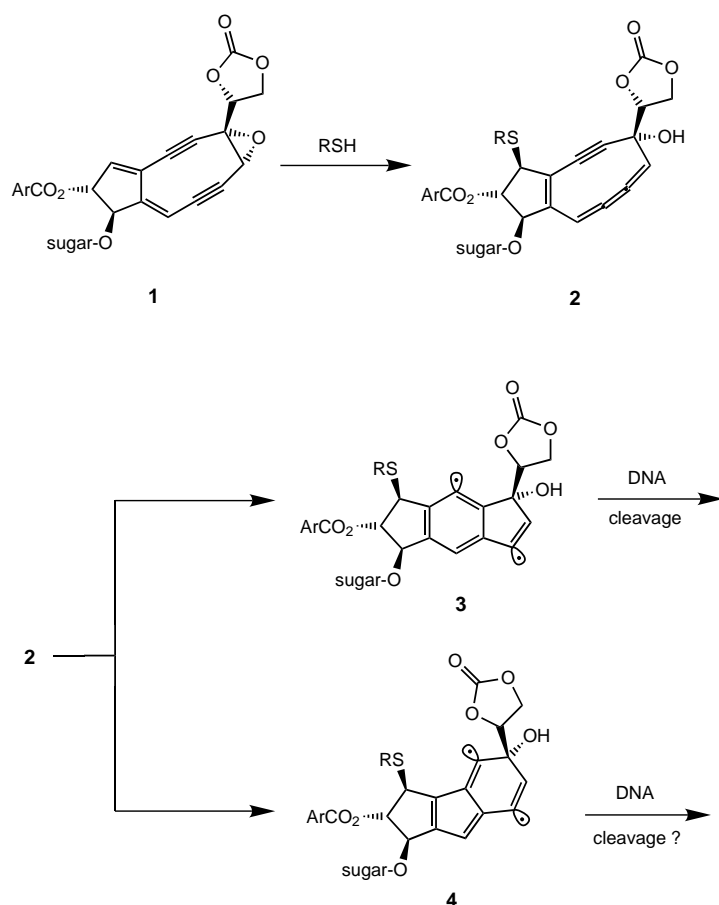
Patrick W. Musch and Bernd Engels*

Neocarzinostatin (NCS) is one representative of the family of natural enediynes that exhibit a high efficacy as antitumor antibiotics.^[1] It consists of a 1:1 complex of an apoprotein and a bioactive non-protein chromophore (**1** in Scheme 1).^[1, 2] In the first step of the mode of action of NCS^[2b, 3] the chromophore **1** is carried to the minor groove of the DNA by the apoprotein which at the same time serves as its stabilizer. After **1** is bound to the DNA the apoprotein is separated off, a stereospecific nucleophilic addition of thiol rearranges **1** to the highly strained enyne-[3]-cumulene **2**.

[*] Prof. Dr. B. Engels, Dipl.-Chem. P. W. Musch
Institut für Organische Chemie
Universität Würzburg
Am Hubland, 97074 Würzburg (Germany)
Fax: (+49) 931-888-4606
E-mail: bernd@chemie.uni-wuerzburg.de

[**] We thank Prof. Dr. M. Schmittel who brought this problem to our attention. P.W.M. thanks the Stiftung Stipendien-Fonds des Verbandes der Chemischen Industrie for a graduate scholarship.

 Supporting information on this contribution is available on the WWW under <http://www.angewandte.com> or from the author.



Scheme 1. Mode of action of the neocarzinostatin chromophore 1.

In the next step the six-membered ring cyclization between the centers C³ and C⁷ leads to the biradical **3**, which through a double hydrogen abstraction from adenine and thymine induces a DNA strand cleavage and as a consequence the cytotoxicity.

While the general course of the mode of action of NCS is clarified, it is still unclear which structural elements are relevant for the high efficacy of NCS. Based on high-level *ab initio* investigations, we present new insight into this topic which is of great interest for the development of new antitumor antibiotics. We first compare the six-membered ring cyclization found in the mode of action of NCS with an alternative five-membered ring cyclization between the C² and C⁷ centers. The latter yields the intermediate **4** instead of **3**; formally both species represent biradicals. For a nine-membered monocyclic enyne-allene, a model compound for the chromophore of NCS (**2**), this alternative route was predicted to be kinetically preferred to the six-membered ring cyclization.^[4] From a comparison of both cyclization modes a new model concerning the tasks of the substituents present in **2** arises. To test this model we discuss the influence of the substituents and the solvent on the kinetics of both cyclization modes. Finally, we study the capability of the arising biradicals for the subsequent hydrogen abstraction leading to the final DNA cleavage. Our investigations provide new insights into the subtle effects which nature uses to obtain powerful antitumor antibiotics. Valuable information for further im-

provements of these substances can be deduced, since some of factors that the limit the efficacy become clear.

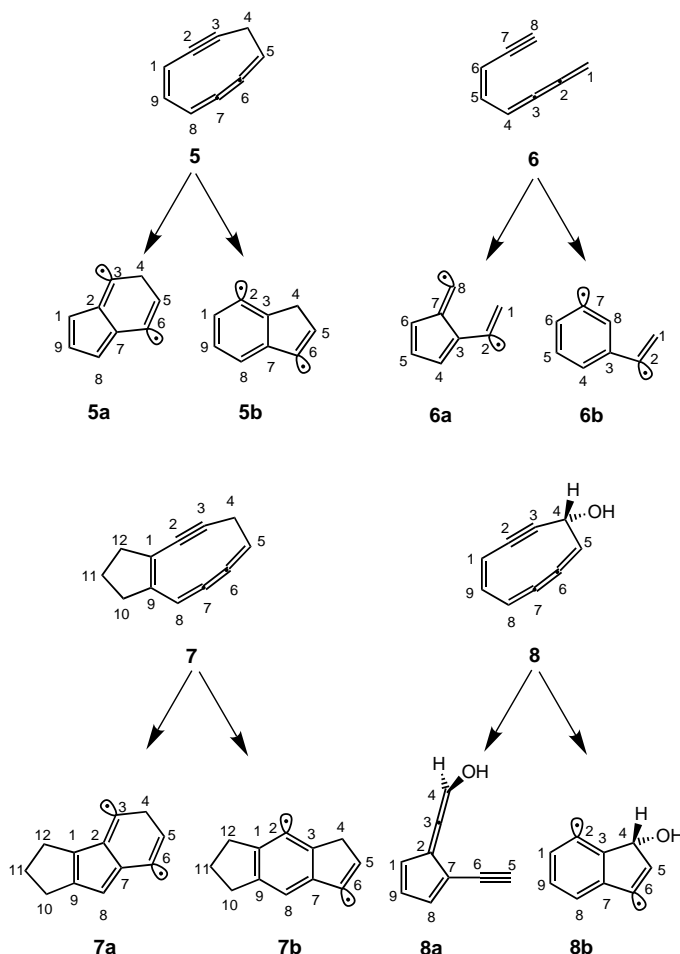
Initial insight into the topics mentioned above can be taken from Table 1, which summarizes the computed activation barriers of the six-membered (C³–C⁷) and of the five-membered (C²–C⁷) ring cyclization for various model compounds.^[5] Our CCSD(T) computations^[6] represent the most reliable approach for the transition states, which possess a

Table 1. Transition states of both possible cyclization modes. All values are in kcal mol^{−1}.

Method	C ² –C ⁷ cyclization ^[a]		C ³ –C ⁷ cyclization ^[b]	
	ΔE^\ddagger	ΔG^\ddagger_{298K}	ΔE^\ddagger	ΔG^\ddagger_{298K}
5	UB3LYP/6-31G(d)	+18.6	+17.6	+21.1
	CCSD(T)/cc-pVDZ	+13.8		+16.5
6	UB3LYP/6-31G(d)	+31.9	+31.9	+22.2
	CCSD(T)/cc-pVDZ	+29.7		+20.1
7 ^[c]	UB3LYP/6-31G(d)	+22.8	+21.4	+22.2
	UB3LYP/6-31G(d)	+19.5	+18.3	+21.6
8	UB3LYP/6-31G(d)	+19.5	+18.3	+21.6
	CCSD(T)/cc-pVDZ	+16.1		+18.3

[a] For **6**: C³–C⁷ cyclization. [b] For **6**: C³–C⁸ cyclization. [c] CCSD(T) calculations could not be performed due to computational limitations.

closed-shell electronic structure. At this level of theory we predict for the parent ring system of the NCS chromophore (**5**; Scheme 2) the C²–C⁷ cyclization to be kineti-



Scheme 2. Model compounds used in this work to investigate ring strain and substituent effects on the cyclization of NCS.

cally preferred to the C³–C⁷ cyclization ($\Delta E^\ddagger(\text{C}^2\text{--C}^7) = +14 \text{ kcal mol}^{-1}$ vs. $\Delta E^\ddagger(\text{C}^3\text{--C}^7) = +17 \text{ kcal mol}^{-1}$), which was found to be the only mode of action in NCS.^[1] Our values obtained for the C³–C⁷ cyclization agree nicely with those calculated by Cramer and Squires employing the BD(T) method.^[7] Compared to **5**, the open-chain compound **6** possesses a considerably smaller activation barrier for the C³–C⁷ cyclization than the C²–C⁷ cyclization ($\Delta E^\ddagger(\text{C}^2\text{--C}^7) = +30 \text{ kcal mol}^{-1}$ vs. $\Delta E^\ddagger(\text{C}^3\text{--C}^7) = +20 \text{ kcal mol}^{-1}$). The comparison between **5** and **6** shows that the shift in the regioselectivity is induced by the ring strain present in **5**. It also indicates that the ring strain is important for the efficacy of **2** since it reduces the activation energy of both cyclization modes considerably. Additionally to **6b**, **5b** represents a biradical with a fixed distance of 3.55 Å between the two radical centers. One can imagine that such a fixed distance is also important for the efficacy of the double hydrogen abstraction in the last step of the mode of action of NCS. However, since in the mode of action of NCS only the C³–C⁷ cyclization is found, our calculations indicate that the substituents present in **2** shift the regioselectivity back to the C³–C⁷ cyclization.

Information on the importance of substituents for the control of the regioselectivity can also be taken from Table 1. The cyclopentene ring in **7** seems to be important for the control of the regioselectivity, since the induced strain increases the activation energy of the C²–C⁷ cyclization more than that of the C³–C⁷ cyclization. A similar trend was found experimentally for enyne-allenes.^[8] In contrast, the OH substituent at C⁴ (**8**) increases both activation barriers by about the same amount (2 kcal mol^{−1}) and therefore does not affect the regioselectivity of the cyclization. However, the substituent completely changes the reaction path of the C²–C⁷ cyclization. Along with the ring closure between C² and C⁷ the ring opens between C⁴ and C⁵ leading to the final product **8a**. In contrast, the C³–C⁷ cyclization still proceeds along a biradical route. Polar solvents also favor the C³–C⁷ cyclization to some extent, since the activation energy of the C³–C⁷ cyclization for **5** and **7** is lowered by approximately 0.5 kcal mol^{−1}, while the activation energy of the C²–C⁷ cyclization is increased by about the same amount. Besides the activation energies also the reaction energies have to be taken into account for the regioselectivity. The reaction energies given in Table 2 show that for the systems considered in this study the C³–C⁷ cyclization is thermodynamically favored.

Our findings suggest that one of the major tasks of the substituents present in the chromophore of NCS is to prevent the five-membered ring cyclization. A possible reason for the control of the regioselectivity can be seen from the computed

reaction energies of both cyclizations and the singlet–triplet gap ($E_{\text{S-T}}$) of both intermediates (Table 2).^[9] The intermediate of the C²–C⁷ cyclization **5a** lies energetically so high that its lifetime is considerably limited by the reverse reaction, which possesses nearly no activation barrier. Additionally, the computed $E_{\text{S-T}}$ value of about 12 kcal mol^{−1} indicates that **5a** does not have distinctive biradical character. In contrast, **5b** lies energetically well below the reactant and represents a true biradical ($E_{\text{S-T}} \approx 4 \text{ kcal mol}^{-1}$). The differences concerning lifetime and biradical character indicate that an efficient hydrogen abstraction, which is the important final step of the mode of action of NCS, will only be possible with **5b**. A similar observation is found for **7**, showing that this behavior seems to represent a general motif for bicyclic enyne-cumulene compounds. The small singlet–triplet gap of the acyclic enyne-cumulene **6a** indicates that the ring strain of the cyclic enyne-cumulene system is responsible for the large values obtained for **5a** and **7a**. Consequently, we expect enyne-cumulene systems in which the C²–C⁷ cyclization is not suppressed to be less efficient antitumor antibiotics.

Our investigations show that the chromophore of NCS represents a fascinating example for natural products in which a subtle balance of various influences leads to the desired result. While the monocyclic enyne-cumulene moiety seems to be important to provide a biradical with a fixed distance between both radical centers and a low activation barrier for the cyclization process, the substituents present in **2** are necessary to prevent the competing C²–C⁷ cyclization.

Received: May 14, 2001 [Z17096]

Table 2. Heat of reactions for both cyclization reactions and singlet–triplet gaps ($E_{\text{S-T}}$) for the corresponding intermediates. All values are in kcal mol^{−1}.

Method	5a	5b	6a	6b	7a	7b
UB3LYP/6-31G(d)	+17.3	+0.8	+16.4	−8.5	+22.2	+2.0
MR-CI + Q/cc-pVDZ	+12.0	−3.7	−	−	−	−
$E_{\text{S-T}}$ (UB3LYP/6-31G(d))	+11.9	+4.5	−3.4	+1.3	+13.0	+4.41

- [1] K. Edo, Y. Koide in *Neocarzinostatin: The Past, the Present and Future of an Anticancer Drug* (Eds.: H. Maeda, K. Edo, N. Ishida), Springer, Tokyo, **1997**, pp. 23–45.
- [2] a) N. Ishida, K. Miyazaki, K. M. Kumagai, K. M. Rikimaru, *J. Antibiot.* **1965**, *18*, 68–76; b) K. C. Nicolaou, W.-M. Dai, *Angew. Chem.* **1991**, *103*, 1453–1481; *Angew. Chem. Int. Ed. Engl.* **1991**, *30*, 1387–1416.
- [3] a) I. H. Goldberg, *Acc. Chem. Res.* **1991**, *24*, 191–198; b) A. G. Myers, *Tetrahedron Lett.* **1987**, *28*, 4493–4496.
- [4] P. R. Schreiner, M. Prall, *J. Am. Chem. Soc.* **1999**, *121*, 8615–8627.
- [5] The geometric parameters of all stationary points were optimized by employing analytical energy gradients within the density functional theory (DFT) framework as implemented in Gaussian98.^[10] For the DFT calculations the B3LYP^[11] functional in connection with a 6-31G(d)^[12] basis set was employed using a spin and space unrestricted approach. All stationary points were analyzed by computed harmonic frequencies at the same level of theory. Vibrational, thermal, and entropy corrections at 298 K were also computed at the B3LYP/6-31G(d) level of theory. To estimate solvent effects the COSMO model^[13] in combination with the B3LYP/6-31G(d) level of theory was employed by using the standard values for water. Transition state energies were obtained by single-point computations employing the more reliable closed-shell coupled cluster (CCSD(T)) approach in conjunction with a cc-pVDZ^[14] basis set. These computations were performed with the MOLPRO 2000.1 package.^[15] The reliability of the CCSD(T) approach was validated by using the T_1 diagnostics. Reaction energies have been computed by using a multireference configuration interaction approach in connection with a Davidson estimate of quadruple excitations (MR-CI + Q) employing a cc-pVDZ basis set as implemented in the DIESEL-MRCI package.^[16] The reference space of the individually selecting MR-CI consisted of up to 27 configuration state functions (CSF) generating a configuration space of up to 223×10^6 CSF. The secular equations to solve were up to the order of 2×10^6 .

- [6] In most cases the CCSD(T) approach represents a more reliable method than DFT. While both methods agree quite nicely in the ΔE^+ values for the open-chain compound **6** larger differences are found for the monocyclic ring systems **5** and **8**. However, while both methods give different absolute values the correct trends are already obtained with DFT.
- [7] C. J. Cramer, R. R. Squires, *Org. Lett.* **1999**, *1*, 215–218.
- [8] a) M. Schmitt, J.-P. Steffen, D. Auer, M. Maywald, *Tetrahedron Lett.* **1997**, *38*, 6177–6180; b) M. Schmitt, J.-P. Steffen, M. Maywald, B. Engels, H. Helten, P. Musch, *J. Chem. Soc. Perkin Trans. 2* **2001**, 1331–1339.
- [9] For **5b** our values for the singlet–triplet splitting agree nicely with those computed at the BD(T) level of theory in ref. [7].
- [10] Gaussian98 (Revision A.7), M. J. Frisch, G. W. Trucks, H. B. Schlegel, G. E. Scuseria, M. A. Robb, J. R. Cheeseman, V. G. Zakrzewski, J. A. Montgomery, R. E. Stratmann, J. C. Burant, S. Dapprich, J. M. Millam, A. D. Daniels, K. N. Kudin, M. C. Strain, O. Farkas, J. Tomasi, V. Barone, M. Cossi, R. Cammi, B. Mennucci, C. Pomelli, C. Adamo, S. Clifford, J. Ochterski, G. A. Petersson, P. Y. Ayala, Q. Cui, K. Morokuma, D. K. Malick, A. D. Rabuck, K. Raghavachari, J. B. Foresman, J. Cioslowski, J. V. Ortiz, A. G. Baboul, B. B. Stefanov, G. Liu, A. Liashenko, P. Piskorz, I. Komaromi, R. Gomperts, R. L. Martin, D. J. Fox, T. Keith, M. A. Al-Laham, C. Y. Peng, A. Nanayakkara, C. Gonzalez, M. Challacombe, P. M. W. Gill, B. G. Johnson, W. Chen, M. W. Wong, J. L. Andres, M. Head-Gordon, E. S. Replogle, J. A. Pople, Gaussian, Inc., Pittsburgh, PA, **1998**.
- [11] a) A. D. Becke, *J. Chem. Phys.* **1993**, *98*, 5648–5652; b) C. Lee, W. Yang, R. G. Parr, *Phys. Rev. B* **1988**, *37*, 785–789.
- [12] W. J. Hehre, R. Ditchfield, J. A. Pople, *J. Chem. Phys.* **1972**, *56*, 2257–2261.
- [13] A. Klamt, G. Schuurmann, *J. Chem. Soc. Perkin Trans. 2* **1993**, 799–805.
- [14] T. H. Dunning, Jr., *J. Chem. Phys.* **1989**, *90*, 1007–1023.
- [15] H.-J. Werner, P. J. Knowles, MOLPRO2000.1, Stuttgart, Birmingham, **2000**.
- [16] M. Hanrath, B. Engels, *Chem. Phys.* **1997**, *225*, 197–202.

Synthetic Inhibitors of Cell Adhesion: A Glycopeptide from E-Selectin Ligand 1 (ESL-1) with the Arabino Sialyl Lewis^x Structure**

Markus Rösch, Holger Herzner, Wolfgang Dippold,
Martin Wild, Dietmar Vestweber, and Horst Kunz*

*Dedicated to Professor Leopold Horner
on the occasion of his 90th birthday*

In the course of the inflammatory cascade, carbohydrate-recognizing receptors are expressed on endothelial cells: P-selectin within some minutes; E-selectin, however, with a

delay of 4–6 hours after the chemotactic stimulus.^[1] The sialyl Lewis^x epitope has been identified as the ligand of both selectins.^[2, 3]

The carbohydrate-binding domain of E-selectin has been investigated by using transfer-NOE NMR spectroscopic experiments on a complex of sialyl Lewis^x with a recombinant E-selectin–IgG fusion protein, molecular modeling studies,^[4] and X-ray crystal structure analysis.^[5] These studies give evidence of the decisive role of the fucose moiety of sialyl Lewis^x in the binding to E-selectin which is mediated by the coordination to a calcium ion.^[5–7] In the case of the natural selectin ligands, other structural elements are evidently also involved in the specific binding. O-Linked N-acetylactosamine saccharides with sialyl Lewis^x determinants are important for the binding of the P-selectin-selective ligand PSGL-1. However, a peptide sequence that is rich in acidic amino acids and contains O-sulfatyl tyrosines also contributes to the binding.^[8, 9] In the case of the endogenous E-selectin adhesion ligand ESL-1, the sialyl Lewis^x ligand is present on an N-glycan.^[10, 11] A contribution of peptide epitopes of ESL-1 has not been reported for the binding to E-selectin, which also plays a role in metastasis^[2b] and, for example, specifically binds to gastrointestinal tumor cells.^[12]

ESL-1 contains five potential N-glycosylation sites.^[11] The amino acid sequences in their neighborhood is conserved to a large extent compared to those of other E-selectin-binding sialoglycoproteins. In this sense, the amino acid sequence 672–681 of ESL-1 **1** around the sequon NLT is identical to the sequence 676–685 of the E-selectin ligand MG160.^[13]

-Gly-Asn-Leu-Thr-Glu-Leu-Glu-Ser-Glu-Asp- **1**

In earlier investigations, a modulating influence of the peptide portion on the carbohydrate recognition was found in the binding of synthetic sialyl Lewis^x glycopeptides to P-selectin^[14] as well as to E-selectin.^[15] As the segment **1** of ESL-1 with its accumulation of acidic amino acids is similar to the binding domain of PSGL-1, we selected this sequence for the construction of a synthetic E-selectin ligand. An additional aim was to find an E-selectin ligand which, like sialyl Lewis^x mimetics,^[16] is stabilized against enzymatic degradation. The fucoside bond is a site for the enzymatic attack on sialyl Lewis^x.^[17] The fucose portion, however, is considered essential for the binding of sialyl Lewis^x to E-selectin (see above).^[4, 5]

It should now be examined whether the α -L-fucoside can be substituted by a β -D-arabinopyranoside, which exposes its three secondary hydroxy groups in the same spatial arrangement as the fucoside. D-Arabinopyranose, however, is absent in mammals and its glycosides should therefore be biologically more stable.

As in the previous syntheses of glycopeptides,^[14, 15] the azido group was used as the protecting group at the anomeric center of the glucosamine unit in the synthesis of the arabino sialyl Lewis^x saccharide.^[18] The in situ anomerization method^[19] was used to glycosylate 4,6-O-benzylidene-N-acetylglucosaminyl azide **2**^[20] with ethylthio-2,3,4-tri-O-benzyl- α , β -D-arabinopyranoside **5** to give β -D-arabinosylglucosamine azide **6** (Scheme 1).

[*] Prof. Dr. H. Kunz, Dr. M. Rösch, Dipl.-Chem. H. Herzner
Institut für Organische Chemie der Universität Mainz
Duesbergweg 10–14, 55128 Mainz (Germany)
Fax: (+49)6131-39-24786
E-mail: hokunz@mail.uni-mainz.de

Prof. Dr. W. Dippold
Naturwissenschaftlich-Medizinisches Forschungszentrum der Universität Mainz und St. Vincenz-Hospital Mainz (Germany)
Dr. M. Wild, Prof. Dr. D. Vestweber
ZMBE—Institut für Zellbiologie, Universität Münster
Von-Esmarch-Str. 56, 48149 Münster (Germany)

[**] This work was supported by the Deutsche Forschungsgemeinschaft and by the Fonds der Chemischen Industrie